

# Application of magnetic activated carbon for combined adsorption with 4-chlorophenol decomposition by hydrogen peroxide oxidation

Le Anh Kien, Ngo Van Thanh Huy, Tran Anh Khoi, Nguyen Thanh Tung,  
Nguyen Thi Thuy, Nguyen Van Linh\*

Vietnam Institute for Technology and Environmental Protection, 57A Truong Quoc Dung Street,  
Ward 10, Phu Nhuan District, Ho Chi Minh City, Viet Nam

\*Email: [linhnguyen40496@gmail.com](mailto:linhnguyen40496@gmail.com)

Received: 22 June 2023; Accepted for publication: 1 November 2023

**Abstract.** This paper presents the synthesis of magnetic activated carbon materials using a coprecipitation method to produce ferromagnetic oxide ( $\text{Fe}_3\text{O}_4$ ) particles attached to the activated carbon surface. The synthetic material is applied to treat 4-chlorophenol in water by an advanced oxidation process using hydrogen peroxide. Modern analysis techniques such as scanning electron microscope (SEM), transmission electron microscopy (TEM), X-ray diffraction (XRD), energy dispersive X-ray (EDX), vibrating sample magnetometer (VSM), specific surface area and pore size distribution (BET/BJH) have been used to analyze the composition and structure of magnetic activated carbon. The results showed that the material sample had  $\text{Fe}_3\text{O}_4$  crystals in the structure with a magnetization of  $8.19 \text{ emu.g}^{-1}$ , a specific surface area BET of  $330.3 \text{ m}^2.\text{g}^{-1}$ , and a total pore volume of  $0.16 \text{ cm}^3.\text{g}^{-1}$ . The ability to oxidize 4-chlorophenol using magnetic activated carbon materials has been studied, and the results indicate that more than 86 % of 4-chlorophenol is decomposed after 60 min with the optimal conditions of pH 3.0,  $\text{H}_2\text{O}_2$  and 4-chlorophenol concentration ratio of 6.8,  $\text{Fe}^{2+}/\text{Fe}^{3+}$  molar ratio of 3:1, and mass fraction of  $\text{Fe}_3\text{O}_4$  on activated carbon of 20 %. This shows the potential for 4-chlorophenol processing in sources discharged with magnetic catalytic materials.

**Keywords:** magnetic activated carbon, 4-chlorophenol, advanced oxidation process.

**Classification numbers:** 2.2.1, 3.4.2.

## 1. INTRODUCTION

The main sources of 4-chlorophenol emissions into the environment are: production of high-molecular compounds, the plant protection chemical industry, etc. Agricultural production also releases 4-chlorophenol into the environment due to the use of pesticides, especially

herbicides [1, 2]. 4-chlorophenol has a very specific odor and is strongly toxic. It has the ability to condense proteins and cause severe burns on the skin [1, 3]. The elimination of chlorophenol compounds needs to apply methods with good reaction performance and post-treatment products at a level that does not harm the organism and humans. The use of advanced oxidation processes is a promising solution to this problem. An advanced oxidation process is defined as oxidative decomposition based on active hydroxyl radicals ( $\bullet\text{OH}$ ) generated during processing. Hydroxyl radical is a strong oxidizing agent, capable of oxidizing all organic compounds, even the most difficult to decompose compounds, turning them into non-toxic inorganic compounds such as  $\text{CO}_2$ ,  $\text{H}_2\text{O}$ , inorganic acids, etc. [4, 5]. This method is considered suitable for the decomposition of persistent organic compounds such as 4-chlorophenol.

Many studies have applied advanced oxidation processes to treat persistent organic compounds with high efficiency. In a study by Yanqiong Wang *et al.* (2022) [5], 4-chlorophenol was treated by an advanced carbon-based heterologous oxidation process. The treatment process achieved a high degradation efficiency with more than 95 % of 4-chlorophenol and 43 % of TOC decomposed after 120 min of reaction. Cezar Catrinescu and colleagues (2012) [4] studied the treatment of 4-chlorophenol by heterologous fenton and photo fenton processes. The results of the study also showed that the 4-chlorophenol content is completely decomposed after 150 min under the optimal conditions: pH value of 3.5, 4-chlorophenol concentration of 20 mg/L, and peroxide consumption of 89 mg/L. Yaoping Guo and colleagues (2017) [6] studied the treatment of 4-chlorophenol using the heterologous fenton process to completely remove 4-chlorophenol and 65.3 % COD after 170 min of reaction at 25 °C, with a catalytic amount of 0.1 g/L, a persulfate to 4-chlorophenol ratio of 24:1 and a mixture pH of 4.4. From the above examples, it can be seen that the application of advanced oxidation processes to remove 4-chlorophenol is completely possible. These studies all achieved high treatment efficiency, but investigating the adsorption process before the oxidation reaction takes place is often overlooked because the carrier has a not too large surface area.

The use of adsorbent materials together with advanced oxidation processes is an effective technology for the treatment of organic pollutants. Heterogeneous catalysis can completely process difficult to decompose organic compounds, but the solution after the reaction has the dissolution of metal ions. It is necessary to apply a carrier material with a large specific surface area to overcome this disadvantage. Activated carbon with a large surface area helps recover iron that participates in the reaction on the surface of the carrier, avoiding dissolution into the post-treatment solution compared to other materials. This study focuses on the synthesis of magnetic activated carbon materials by coprecipitation in an aerobic environments. The treatment of 4-chlorophenol was investigated as an oxidation reaction combined with adsorption according to the influencing factors: pH of solution, concentration ratio of  $\text{H}_2\text{O}_2$  and 4-chlorophenol,  $\text{Fe}^{2+}/\text{Fe}^{3+}$  ratio, and mass fraction of  $\text{Fe}_3\text{O}_4$  on activated carbon. The research has demonstrated that magnetic activated carbon can be applied to treat 4-chlorophenol with high treatment efficiency and magnetic recovery after processing.

## 2. MATERIALS AND METHODS

### 2.1. Materials

Chemicals used to synthesize magnetic activated carbon include: activated carbon (0.5-1 mm particle size powder - China), iron II chloride tetrahydrate ( $\text{FeCl}_2 \cdot 4\text{H}_2\text{O}$  99.5 % - China), iron III chloride hexahydrate ( $\text{FeCl}_3 \cdot 6\text{H}_2\text{O}$  99.7 % - China), ammonia solution ( $\text{NH}_3$  28-30 % -

China), acid hydrochloric (HCl 36.5 % - China), and ethanol (C<sub>2</sub>H<sub>5</sub>OH 99 % - China). Deionized water (DI) was purified through a Milipore system with a resistivity of 18.2 MΩ/cm.

## **2.2. Synthesis of magnetic activated carbon**

Activated carbon (AC) was pre-treated with 0.1 M HCl solution to remove ash impurities, then washed and dried at 100 °C. 10 g of activated carbon treated above was impregnated with a mixture of FeCl<sub>2</sub> and FeCl<sub>3</sub> (at a molar ratio of 1:2) [7]. The mixture was stirred using a magnetic stirrer and kept at a temperature of 70 - 80 °C, under oxygen deprivation conditions using a nitrogen gas flow to expel all the oxygen in the air from the reaction mixture. The mixture was then coprecipitated with 20 mL of NH<sub>3</sub> solution (28 - 30 %) under oxygen deprivation conditions, and continued to be stirred at a temperature of 70 - 80 °C. The reaction mixture was aged at room temperature (25 °C) for 24 h, then filtered to wash the solid mixture with ethanol and deionized water until the wash water had a neutral pH and then the solid was put into an oven at 70 °C for 12 h, resulting in magnetic activated carbon (MAC).

## **2.3. Characterization techniques**

Surface morphological characteristics, properties and composition of materials were analyzed by modern methods such as scanning electron microscope - SEM (Hitachi S-4800, Japan), transmission electron microscopy - TEM (JEM-2100F, Japan), X-ray diffraction - XRD (D2Phaser, Bruker, Germany), energy dispersive X-ray - EDX (Shimadzu EDX-LE, Japan), vibrating sample magnetometer - VSM (8600 Series VSM, LakeShore, United Kingdom). Specific surface area and pore size distribution (BET/BJH) were determined from a N<sub>2</sub> adsorption-desorption at 77.35 K (PMI's BET Sorptometer, India) [8].

## **2.4. Adsorption and fenton oxidation reaction**

Adsorption studies considering factors such as solution pH and adsorption time, conducted under catalytic initial conditions with 0.3 g/L of catalyst and a 4-chlorophenol concentration of 100 mg/L. The oxidation reaction of 4-chlorophenol was carried out in combination with the adsorption of 4-chlorophenol at its concentration of 100 mg/L pollutant solution and a catalyst concentration of 0.3 g/L. After the adsorption reached equilibrium, H<sub>2</sub>O<sub>2</sub> was added to the mixture to trigger the 4-chlorophenol decomposition reaction to take place. Factors affecting the 4-chlorophenol oxidation reaction included H<sub>2</sub>O<sub>2</sub> concentration, pH of solution, Fe<sup>2+</sup>/Fe<sup>3+</sup> molar ratio and mass fraction of Fe<sub>3</sub>O<sub>4</sub> on activated carbon. The H<sub>2</sub>O<sub>2</sub> concentration varied according to the ratio of the initial concentration of hydrogen peroxide to 4-chlorophenol, [H<sub>2</sub>O<sub>2</sub>]/[4-CP] in the range from 0 to 10.2, the pH value of the solution from 2 to 7 (adjusted with 1 mol/L HCl and 1 mol/L NaOH), the Fe<sup>2+</sup>/Fe<sup>3+</sup> molar ratio on activated carbon from 3/1 to 1/3, and the mass fraction of Fe<sub>3</sub>O<sub>4</sub> on activated carbon from 5 to 25 %. After the reaction, the solid fraction was separated from the solution by a magnetic field and the remaining amount of 4-chlorophenol was analyzed by high performance liquid chromatography equipped with a C18 column (4.6 × 150 mm, 5.0 μm) and a photodiode array detector (PDA). The mobile phase was a binary mixture of methanol and water (70 %/30 %, v/v) at a flow rate of 1 mL/min [5].

# **3. RESULTS AND DISCUSSION**

## **3.1. Characteristics of the magnetic activated carbon**

The morphological characteristics, surface properties and composition of activated carbon and Fe<sub>3</sub>O<sub>4</sub>/activated carbon materials were analyzed using SEM images, TEM images, XRD pattern, and EDX spectrum. The results obtained are shown in Figure 1.

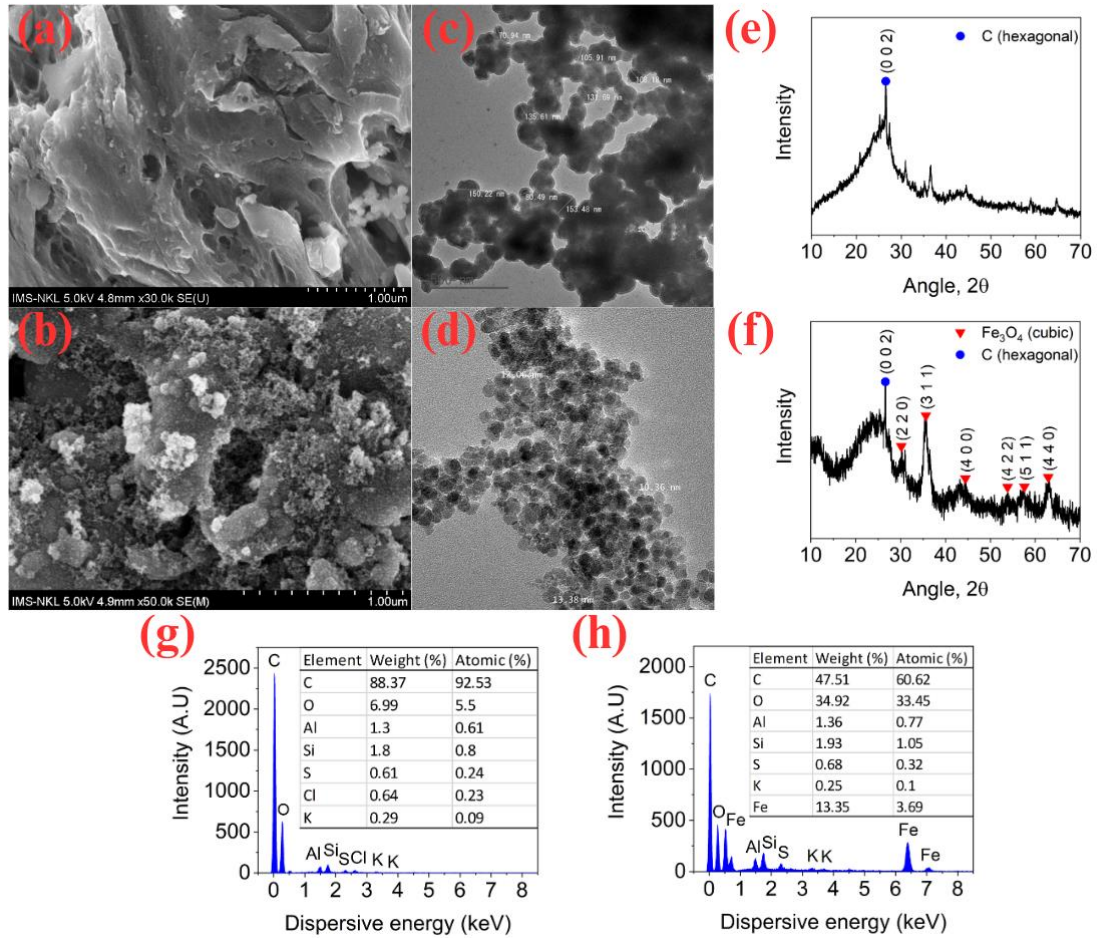


Figure 1. Morphological characteristics of (a) SEM image of AC; (b) SEM image of MAC; (c) TEM image of AC; (d) TEM image of MAC; (e) XRD pattern of AC; (f) XRD spectrum of MAC; (g) EDX spectrum of AC; and (h) EDX spectrum of MAC.

SEM images in Figures 1a and 1b show the difference between the rough surface of magnetic activated carbon and the surface of activated carbon. TEM images in Figures 1c and 1d show that Fe<sub>3</sub>O<sub>4</sub> nanoparticles on the activated carbon surface are 10-15 nm in size. From the XRD spectrograph on Figures 1e and 1f, it can be seen that the synthesized magnetic iron oxide nanoparticles have a cubic crystal configuration (typical spinel structure) with an edge size of 8.37 Å attached to the pore surface of activated carbon with a hexagonal configuration of graphite crystals with a space group structure of P63/MMC (materials studio). The diffraction peaks show miller plane characteristic of magnetic iron oxide (220), (311), (400), (422), (511), (440) along with plane (002) characteristic of hexagonal structure of carbon [9]. The EDX spectra in Figures 1g and 1h show the difference between magnetic activated carbon and activated carbon according to the elemental composition of Fe and O due to the amount of iron

oxide on the surface increasing their density. Magnetic activated carbon surfaces that do not contain Cl can be explained by the fact that after being pre-treated with HCl, they were released in a basic medium of  $\text{NH}_4\text{OH}$  and washed into an aqueous solution.

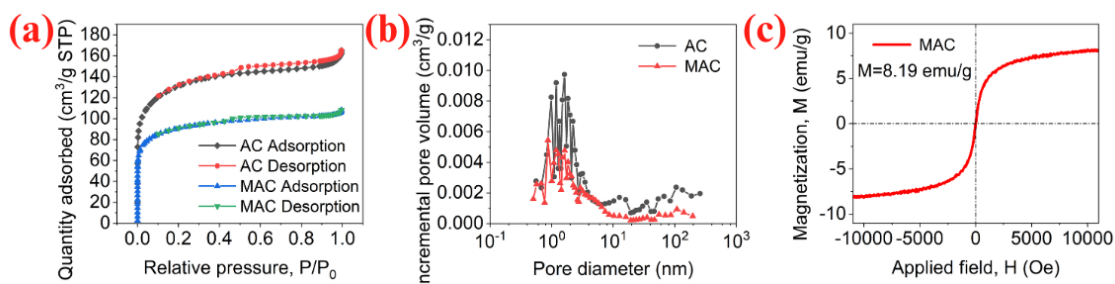


Figure 2. Surface and magnetic properties: (a)  $\text{N}_2$  adsorption-desorption isotherm; (b) pore size distribution; and (c) vibrating sample magnetometry.

The analysis of specific surface area and pore size distribution of activated carbon and magnetic activated carbon using the BET-BJH method (Figures 2a and 2b) indicates that the nitrogen adsorption-desorption isotherm corresponds to Type II (IUPAC) [10], which is characteristic of microporous structures and is consistent with the Barrett-Joyner-Halenda (BJH) pore size distribution.

Table 1. Pore structure properties of activated carbon and magnetic activated carbon.

Material	Specific surface area	Specific surface micropore area	Average pore diameter	Pore volume
	$\text{m}^2 \cdot \text{g}^{-1}$	$\text{m}^2 \cdot \text{g}^{-1}$	nm	$\text{cm}^3 \cdot \text{g}^{-1}$
Activated carbon	469.9	283.5	1.86	0.25
$\text{Fe}_3\text{O}_4$ /Activated carbon	330.3	219.1	1.56	0.16

Activated carbon and magnetic activated carbon do not have a closed-loop form at pressures below 0.1. This also shows the predominant appearance of micropore structures. The total pore volume and specific surface area were somewhat reduced due to the presence of  $\text{Fe}_3\text{O}_4$  crystals mounted on the surface, the amount of  $\text{Fe}_3\text{O}_4$  crystals on the activated carbon surface was also spread evenly over the surface, as evidenced by the pore size distribution graph with uniform size loss spread across all pore value ranges. The results of measuring specific surface area and average pore size are shown through the parameters in Table 1. The magnetic activated carbon curve is shown in Figure 2c. The magnetization properties of the magnetic activated carbon material were analyzed using a vibrating sample magnetometer at 300 K. Magnetic activated carbon exhibits superparamagnetic properties with a saturation magnetization (M) of 8.19 emu/g.

### 3.2. Adsorption of 4-chlorophenol by magnetic activated carbon

#### 3.2.1. Adsorption kinetics

The results of the adsorption kinetic curve study are shown in Figure 3. The study was conducted on the adsorption of 4-chlorophenol from a solution with a concentration of  $100 \text{ mg} \cdot \text{L}^{-1}$  and a pH value of 6.

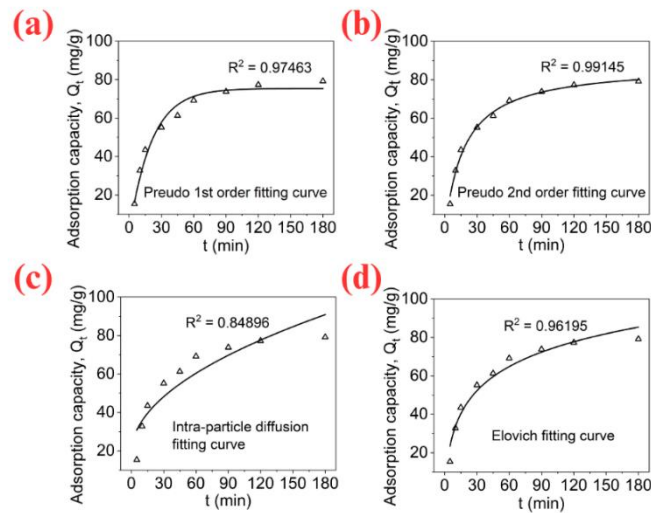


Figure 3. Adsorption kinetic models: (a) pseudo first order; (b) pseudo second order; (c) intra particle diffusion; and (d) elovich.

From Figure 3, it can be seen that the adsorption of 4-chlorophenol gradually reaches saturation state when the reaction time is 180 min, achieving an adsorption capacity of  $79.2 \text{ mg.g}^{-1}$ . This value is used to conduct adsorption isotherm research experiments in the following sections. The equilibrium adsorption capacity of magnetic activated carbon is only  $79.2 \text{ mg.g}^{-1}$ . This is explained by the structure of magnetic activated carbon whose surface is covered with magnetic iron nanoparticles, which reduces the specific surface area, so the adsorption capacity is significantly reduced [2]. Pseudo first order, pseudo second order, intra particle diffusion, and elovich kinetic models were selected to conduct the study, showing that the adsorption of 4-chlorophenol on magnetic activated carbon follows a pseudo second order model with an  $R^2$  coefficient of 0.99145 with a maximum adsorption capacity calculated from the model of  $87.9 \text{ mg.g}^{-1}$ .

### 3.2.2. Adsorption isotherms

The results of the adsorption isotherm study are shown in Figure 4. The study was conducted with varying concentrations of 4-chlorophenol (5, 10, 15, 25, 50 and  $100 \text{ mg.L}^{-1}$ ) at a pH value of 6 during a reaction time of 180 min.

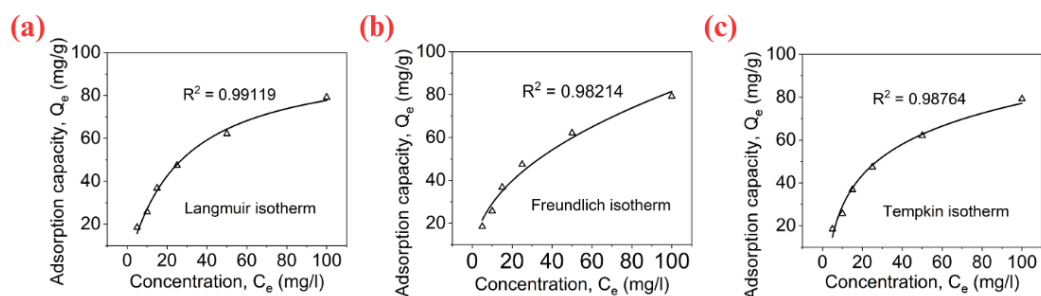


Figure 4. Adsorption isotherm models: (a) Langmuir isotherm; (b) Freundlich isotherm; and (c) Tempkin isotherm.

From Figure 4, it can be seen that the adsorption capacity increases rapidly when the concentration varies from 5 to 25 mg.L<sup>-1</sup> and decreases gradually when the concentration increases to 100 mg.L<sup>-1</sup>. Isotherm adsorption study with Langmuir, Freundlich, Tempkin models show that the adsorption process of 4-chlorophenol on magnetic activated carbon follows the Langmuir model with an R<sup>2</sup> coefficient of 0.9912 and a maximum adsorption capacity of 98.1 mg.g<sup>-1</sup> [10].

### 3.3. Fenton oxidation reaction of 4-chlorophenol by hydrogen peroxide with magnetic activated carbon

The study on 4-chlorophenol oxidation reaction was conducted in conjunction with the adsorption process, peroxide was used to activate the oxygenation reaction with influencing factors including pH, concentration ratio of H<sub>2</sub>O<sub>2</sub> and 4-chlorophenol, mass fraction of Fe<sub>3</sub>O<sub>4</sub> on activated carbon, and Fe<sup>2+</sup>/Fe<sup>3+</sup> ratio on magnetic activated carbon.

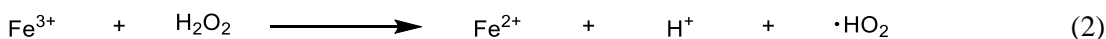
#### 3.3.1. Effect of solution pH and initial hydrogen peroxide concentration

The results of the study on the effect of pH are shown in Figure 5. The 4-chlorophenol degradation process was investigated using the pseudo first order and pseudo second order models, both achieving highly consistent coefficients (R<sup>2</sup> > 0.92), and the 4-chlorophenol degradation was most consistent with the quadratic model with a correlation coefficient of R<sup>2</sup> > 0.96 [11, 12]. The greatest degradation efficiency achieved at pH 3 is 94 % with a reaction rate constant of k = 0.00127 mg<sup>-1</sup>.L.min<sup>-1</sup> and a correlation coefficient of R<sup>2</sup> = 0.9836. Therefore, this model is suitable for assessing the degradation level of 4-chlorophenol.

Table 2. Fitting parameters for the oxidation rate data of 4-chlorophenol at different pHs of solution.

pH of solution	Pseudo first order		Pseudo second order	
	k (min <sup>-1</sup> )	R <sup>2</sup>	k (mg <sup>-1</sup> .L.min <sup>-1</sup> )	R <sup>2</sup>
2	0.01390	0.9389	0.000504	0.9901
3	0.02012	0.9218	0.001270	0.9836
4	0.00908	0.9636	0.000221	0.9951
5	0.00466	0.9545	0.000082	0.9733
6	0.00251	0.9573	0.000039	0.9654
7	0.00166	0.9609	0.000024	0.9647

The decomposition of 4-chlorophenol increases when pH is reduced from 7 to 3 because at high pH the production of hydroxyl radicals (•OH) is reduced (Eq. 1). But when pH is reduced from 3 to 2, the rate is reduced because low pH hinders the reduction of Fe<sup>3+</sup> to Fe<sup>2+</sup> reducing the rate of H<sub>2</sub>O<sub>2</sub> activation (Eqs. 2, 3), thus leading to a decrease in the production of hydroxyl radicals (•OH) [13].



The results of the study on the effect of the ratio of H<sub>2</sub>O<sub>2</sub> concentration to initial 4-chlorophenol concentration at the optimal pH value of 3 are shown in Figure 5. The decomposition of 4-chlorophenol by H<sub>2</sub>O<sub>2</sub> using magnetic activated carbon achieves high efficiency progressively, with the greatest value obtained when the concentration ratio of H<sub>2</sub>O<sub>2</sub> and 4-chlorophenol is 6.8.

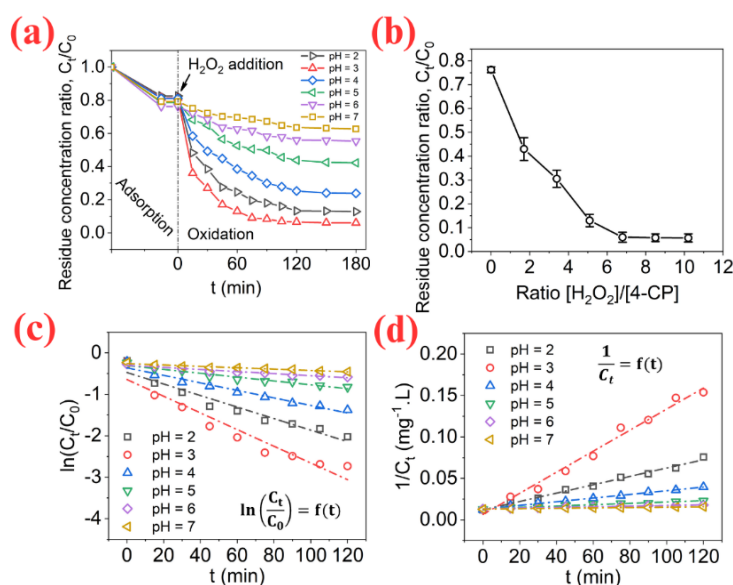


Figure 5. Effect of: (a) pH and (b) concentration ratio of peroxide and 4-chlorophenol; kinetic models of: (c) pseudo first order and (d) pseudo second order at different pHs.

The processing efficiency increases as the concentration of  $H_2O_2$  increases, but if the value is too high, there is a problem of producing too much precipitated iron because hydroxyl groups (OH) are produced with hydroxyl radicals ( $\bullet OH$ ). The optimal concentration ratio of  $H_2O_2$  and 4-chlorophenol for the experiment is 6.8, which is used for further studies.

### 3.3.2. Effect of mass fraction of $Fe_3O_4$ and $Fe^{2+}/Fe^{3+}$ ratio on magnetic activated carbon

The results of the study on the effect of mass fraction (% w/w) of  $Fe_3O_4$  on activated carbon with its values varying from 5 to 25 % are shown in Figures 6a, 6b.

For different iron oxide ratios and with a decomposition efficiency greater than 50%, the 4-chlorophenol decomposition rate studied by the models all achieve a high matching coefficient ( $R^2 > 0.88$ , Table 4). The decomposition of 4-chlorophenol is consistent with the second order pseudo model with a coefficient of  $R^2 > 0.97$ . The mass fraction of  $Fe_3O_4$  on magnetic activated carbon is 20 % for pseudo second order with constant  $k$  of  $0.00127 \text{ mg}^{-1} \cdot \text{L} \cdot \text{min}^{-1}$  ( $R^2 = 0.9857$ ) reaching an efficiency of 94 %. Increasing the mass fraction of  $Fe_3O_4$  on magnetic activated carbon from 5 to 20 % results in an increase in the reaction rate.

Table 3. Fitting parameters for the oxidation rate data of 4-chlorophenol with different mass fractions of  $Fe_3O_4$  on activated carbon.

Mass fraction	Pseudo first order		Pseudo second order	
	$k \text{ (min}^{-1}\text{)}$	$R^2$	$k \text{ (mg}^{-1} \cdot \text{L} \cdot \text{min}^{-1}\text{)}$	$R^2$
5 %	0.00731	0.87	0.00018	0.9452
10 %	0.00943	0.8817	0.00027	0.9714
15 %	0.01272	0.9046	0.00047	0.9899
20 %	0.02012	0.9218	0.00127	0.9857
25 %	0.01607	0.9486	0.00067	0.9861

The increased content of iron oxide provides additional  $\text{Fe}^{2+}$  ions that accelerate the activation of  $\text{H}_2\text{O}_2$ . The degradation efficiency is reduced due to the excess  $\text{Fe}^{2+}$  ions reacting with hydroxyl radicals when the amount of iron oxide is higher than the optimal value according to Eq. 4 [14].

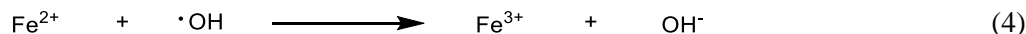


Table 4. Fitting parameters for the oxidation rate data of 4-chlorophenol with different  $\text{Fe}^{2+}/\text{Fe}^{3+}$  ratios on  $\text{Fe}_3\text{O}_4$ .

$\text{Fe}^{2+}/\text{Fe}^{3+}$ ratio	Pseudo first order		Pseudo second order	
	k ( $\text{min}^{-1}$ )	$R^2$	k ( $\text{mg}^{-1} \cdot \text{L} \cdot \text{min}^{-1}$ )	$R^2$
3:1	0.02389	0.9539	0.00212	0.9295
2:1	0.02264	0.9717	0.00162	0.9410
1:1	0.01597	0.9171	0.00072	0.9925
1:2	0.02012	0.9218	0.00127	0.9856
1:3	0.01082	0.8744	0.00035	0.9731

The results of the study on the effect of mass fraction (% w/w) of  $\text{Fe}_3\text{O}_4$  on activated carbon with its values varying from 5 to 25 % are shown in Figures 6c, 6d.

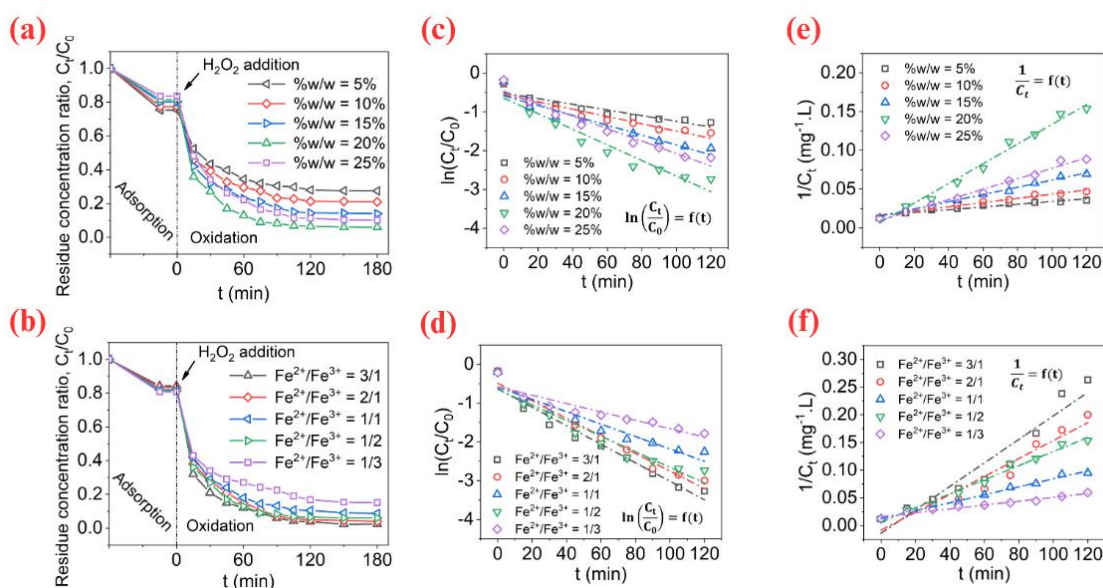


Figure 6. Effect of: (a) mass fraction of  $\text{Fe}_3\text{O}_4$  and (b)  $\text{Fe}^{2+}/\text{Fe}^{3+}$  ratio on magnetic activated carbon; kinetic models of: (c) pseudo first order; (e) pseudo second order with different mass fractions of  $\text{Fe}_3\text{O}_4$  and (d) pseudo first order and (f) pseudo second order with different  $\text{Fe}^{2+}/\text{Fe}^{3+}$  ratios.

The decomposition efficiency for different  $\text{Fe}^{2+}/\text{Fe}^{3+}$  ratios all reaches over 80 %, of which the highest efficiency is 97 % at the  $\text{Fe}^{2+}/\text{Fe}^{3+}$  ratio of 3:1. For the ratio of  $\text{Fe}^{2+}$  and  $\text{Fe}^{3+}$  components, the higher the amount of  $\text{Fe}^{2+}$  will shift the equilibrium of reaction (1) forward at a greater rate because the activity of  $\text{Fe}^{2+}$  is directly proportional to the rate of oxidation reactions.

Evaluating the decomposition of 4-chlorophenol using kinetic models achieving a high coefficient of conformity ( $R^2 > 0.87$ ) further increases the model's conformity. The degradation is best suited to the pseudo second order model ( $R^2 > 0.94$ ) with the reaction rate constant increasing with increasing  $Fe^{2+}$  (from 0.00035 to 0.00212  $mg^{-1}.L.min^{-1}$ ), and the slope of the characteristic equations shows the great influence of the  $Fe_3O_4$  catalyst composition.

### 3.4. Mechanism of fenton oxidation reaction of 4-chlorophenol

This section presents the research results on the mechanism of 4-chlorophenol decomposition by hydroxyl radicals ( $\bullet OH$ ) clarifying the cause of 4-chlorophenol degradation after adding peroxide ( $H_2O_2$ ). The degradation of 4-chlorophenol by magnetic activated carbon catalyst is accelerated when  $H_2O_2$  is added due to the addition of hydroxyl radicals ( $\bullet OH$ ) to the benzene ring structure of 4-chlorophenol, which causes the ring to open creating open circuit structures before the final products of oxidation like  $CO_2$ ,  $H_2O$  and  $Cl^-$  are obtained [13, 14]. The study of the oxidation reaction mechanism can partly explain the rapid rate of the 4-chlorophenol degradation within the first 60 minutes after adding peroxide. The reaction mechanism is shown in Figure 7 [14].

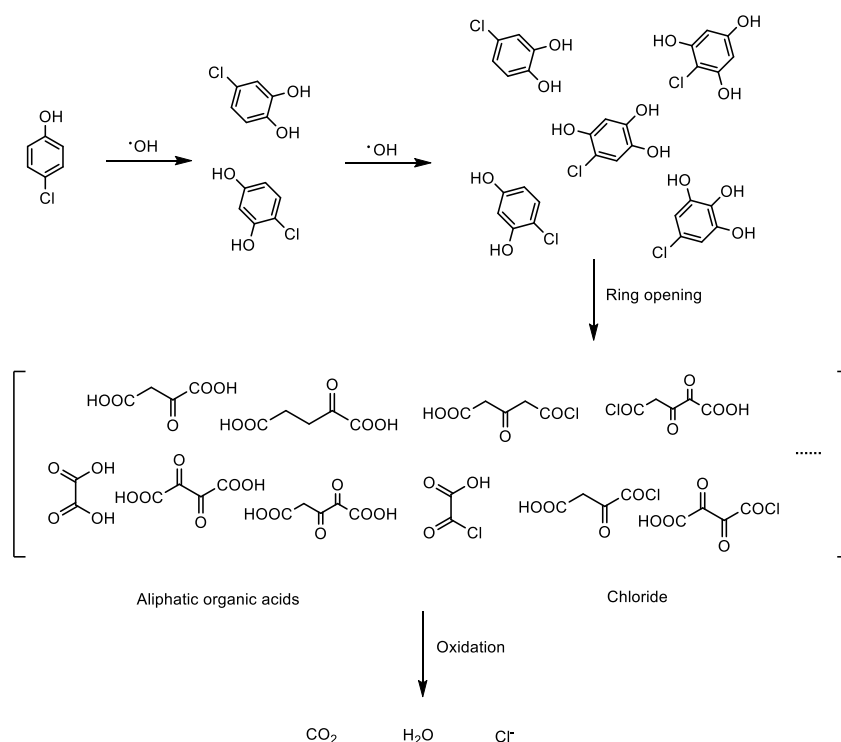


Figure 7. Mechanism of oxidation reaction [14].

According to the mechanism presented above, due to the double conjugate structure in the benzene ring and the  $\pi$ - $\pi$  conjugate system, single-molecule free radical addition reactions preferentially occur. Because of the high reaction rate, the 4-chlorophenol concentration initially decreased markedly along with an increase in total organic carbon index and the concentration of intermediate products such as 4-chlorocatechol and 4-chloro 2,6-dihydroxy phenol, etc. This is

followed by ring opening due to an attack on the -C=C- double bond of the hydroxyl radical ( $\bullet\text{OH}$ ) creating lower carbon chain structures (containing 2, 4, 5 carbon atoms) and organic chloride isomers [6]. When the structure is transformed from a ring to a branched chain, it is a favorable condition for the chain cleavage reaction into smaller molecules that lead to the formation of  $\text{CO}_2$  and  $\text{H}_2\text{O}$  molecules which are characteristic products of the complete oxidation of organic substances and some amount of chloride ( $\text{Cl}^-$ ) formed from the composition of the original 4-chlorophenol.

#### 4. CONCLUSIONS

In this study, magnetic activated carbon materials were successfully synthesized by the coprecipitation method on the carrier. Magnetic iron nanoparticles are formed with a characteristic spinel structure with high dispersion, specific surface area of  $330.3 \text{ m}^2.\text{g}^{-1}$ , average pore diameter of 1.56 nm, total pore volume of  $0.16 \text{ cm}^3.\text{g}^{-1}$ , and saturation magnetization ( $M$ ) of  $8.19 \text{ emu}.\text{g}^{-1}$ . Research on the decomposition of 4-chlorophenol by magnetic activated carbon was conducted using the combined adsorption oxidation method. The results of studying the adsorption kinetics of 4-chlorophenol onto magnetic activated carbon are most consistent with the pseudo second order model with an  $R^2$  coefficient of 0.9915, the adsorption isotherm follows the Langmuir model with an  $R^2$  coefficient of 0.9912. The oxidation of 4-chlorophenol is conducted immediately after the adsorption process with peroxide ( $\text{H}_2\text{O}_2$ ), with the following optimal conditions: solution pH of 3.0,  $\text{H}_2\text{O}_2$  and 4-chlorophenol concentration ratio of 6.8,  $\text{Fe}^{2+}/\text{Fe}^{3+}$  molar ratio of 3:1, and mass fraction of  $\text{Fe}_3\text{O}_4$  on activated carbon of 20 % with the greatest degradation efficiency achieved at 97 %. The oxidation kinetics is discussed with the matching of the 2nd order pseudo model with a high correlation coefficient ( $R^2 > 0.94$ ). The oxidation mechanism is discussed to find the law of 4-chlorophenol reduction proposed by a series of free radical addition, ring opening, and ultimately aliphatic organic acids, forming the end products like carbon dioxide, water and chloride. The study results show the potential of magnetic activated carbon materials with high catalytic activity to treat persistent organic compounds.

**Acknowledgements.** This research was funded by the Vietnam Institute for Tropical Technology and Environmental Protection (No. DTVCBT.80-2/VNĐMT).

**CRedit authorship contribution statement.** Le Anh Kien: Formal analysis, supervision. Ngo Van Thanh Huy: Formal analysis, supervision. Tran Anh Khoi: Methodology, experiment. Nguyen Thanh Tung: Formal analysis, experiment. Nguyen Thi Thuy: Formal analysis, Supervision. Nguyen Van Linh: Methodology, experiment, supervision, completing the manuscript.

**Declaration of competing interest.** The authors declare that they have no known competing financial interests or personal relationships that could have appeared to influence the work reported in this paper.

#### REFERENCES

1. Wei D., Wang Y., Wang X., Li M., Han F., Ju L., Zhang G., Shi L., Li K., Wang B. - Toxicity assessment of 4-chlorophenol to aerobic granular sludge and its interaction with extracellular polymeric substances, *Journal of Hazardous Materials* **289** (2015) 101-107. <https://doi.org/10.1016/j.jhazmat.2015.02.047>
2. Shen T., Wang P., Hu L., Hu Q., Wang X., Zhang G. - Adsorption of 4-chlorophenol by wheat straw biochar and its regeneration with persulfate under microwave irradiation,

- Journal of Environmental Chemical Engineering **9** (2021) 105353. <https://doi.org/10.1016/j.jece.2021.105353>
3. Zada A., Khan M., Khan M. A., Khan Q., Habibi-Yangjeh A., Dang A., Maqbool M. - Review on the hazardous applications and photodegradation mechanisms of chlorophenols over different photocatalysts, *Environmental Research* **195** (2021) 110742. <https://doi.org/10.1016/j.envres.2021.110742>
  4. Catrinescu C., Arsene D., Apopei P., Teodosiu C. - Degradation of 4-chlorophenol from wastewater through heterogeneous Fenton and photo-Fenton process, catalyzed by Al-Fe PILC, *Applied Clay Science* **58** (2012) 96-101. <https://doi.org/10.1016/j.clay.2012.01.019>
  5. Wang Y., Wang H., Wang L., Cai B., Chen H. - Removal of high-concentration 4-Chlorophenol (4-CP) in wastewater using carbon-based heterogeneous catalytic oxidation: Performance and mechanism, *Journal of Cleaner Production* **346** (2022) 131176. <https://doi.org/10.1016/j.jclepro.2022.131176>
  6. Guo Y., Zeng Z., Li Y., Huang Z., Yang J. - Catalytic oxidation of 4-chlorophenol on in-situ sulfur-doped activated carbon with sulfate radicals, *Separation and Purification Technology* **179** (2017) 257-264. <https://doi.org/10.1016/j.seppur.2017.02.006>
  7. Hadi S., Taheri E., Amin M. M., Fatehizadeh A., Aminabhavi T. M. - Adsorption of 4-chlorophenol by magnetized activated carbon from pomegranate husk using dual stage chemical activation, *Chemosphere* **270** (2021) 128623. <https://doi.org/10.1016/j.chemosphere.2020.128623>
  8. Zhu R., Xia J., Zhang H., Kong F., Hu X., Shen Y., Zhang W. H. - Synthesis of magnetic activated carbons from black liquor lignin and Fenton sludge in a one-step pyrolysis for methylene blue adsorption, *Journal of Environmental Chemical Engineering* **9** (2021) 106538. <https://doi.org/10.1016/j.jece.2021.106538>
  9. Ilyas S., Abdullah B., Tahir D. J. N. S. - Nano-Objects -X-ray diffraction analysis of nanocomposite Fe<sub>3</sub>O<sub>4</sub>/activated carbon by Williamson-Hall and size-strain plot methods, **20** (2019) 100396. <https://doi.org/10.1016/j.nanoso.2019.100396>
  10. Tang X., Ripepi N., Stadie N. P., Yu L., Hall M. R. J. F. - A dual-site Langmuir equation for accurate estimation of high pressure deep shale gas resources, **185** (2016) 10-17. <https://doi.org/10.1016/j.fuel.2016.07.088>
  11. Ferreiro C., Sanz J., Villota N., de Luis A., Lombraña J. I. - Kinetic modelling for concentration and toxicity changes during the oxidation of 4-chlorophenol by UV/H<sub>2</sub>O<sub>2</sub>, *Scientific Reports* **11** (2021) 15726. <https://doi.org/10.1038/s41598-021-95083-7>
  12. Murcia M., Gómez M., Gómez E., Gómez J. L., Hidalgo A. M., Christofi N. - A new substrate and by-product kinetic model for the photodegradation of 4-chlorophenol with KrCl exciplex UV lamp and hydrogen peroxide, *Chemical Engineering Journal* **187** (2012) 36-44. <https://doi.org/10.1016/j.cej.2012.01.069>
  13. Wang J., Wang S. - Reactive species in advanced oxidation processes: Formation, identification and reaction mechanism, *Chemical Engineering Journal* **401** (2020) 126158. <https://doi.org/10.1016/j.cej.2020.126158>
  14. Cheng R., Li G. Q., Cheng C., Shi L., Zheng X., Ma Z. - Catalytic oxidation of 4-chlorophenol with magnetic Fe<sub>3</sub>O<sub>4</sub> nanoparticles: mechanisms and particle transformation, *RSC advances* **5** (2015) 66927-66933. DOI: [10.1039/C5RA10433E](https://doi.org/10.1039/C5RA10433E)